## Title
Force Field for Water over Pt(111): Development, Assessment, and Comparison



## Journal
Journal of Chemical Theory and Computation, 14(6)

## ISSN
1549-9618

## Authors
Steinmann, Stephan N
De Morais, Rodrigo Ferreira
Götz, Andreas W
et al.

## Publication Date
2018-06-12

## DOI
10.1021/acs.jctc.7b01177

Peer reviewed

# A Force Field for Water over Pt(111): Development, Assessment and Comparison

Stephan N. Steinmann,[*,†] Rodrigo Ferreira De Morais,[†] Andreas W. Götz,[*,‡] Paul Fleurat-Lessard,[¶] Marcella Iannuzzi,[§] Philippe Sautet,[‖,⊥] and Carine Michel[†]

†*Univ Lyon, Ecole Normale Supérieure de Lyon, CNRS Université Lyon 1, Laboratoire de Chimie UMR 5182, 46 allée d'Italie, F-69364, LYON, France*

‡*San Diego Supercomputer Center, University of California San Diego, La Jolla, CA 92093, USA.*

¶*Institut de Chimie Moléculaire de l'Université de Bourgogne (ICMUB, UMR 6302, CNRS), Université de Bourgogne Franche-Comté, 9 Avenue Alain Savary, 21078 Dijon, France.*

§*Institut für Chemie, University of Zurich, Winterthurerstrasse 190, CH-8057 Zurich, Switzerland.*

‖*Department of Chemical and Biomolecular Engineering, University of California Los Angeles, Los Angeles, CA 90095, USA.*

⊥*Department of Chemistry and Biochemistry, University of California Los Angeles, Los Angeles, CA 90095, USA.*

E-mail: stephan.steinmann@ens-lyon.fr; agoetz@sdsc.edu

**Abstract**

Metal/water interfaces are key in many natural and industrial processes, such as corrosion, atmospheric or environmental chemistry. Even today, the only practical approach to simulate large interfaces between a metal and water is to perform force field simulations. In this work, we propose a novel force field, GAL17, to describe the

interaction of water and a Pt(111) surface. GAL17 builds on three terms: (i) a standard Lennard-Jones potential for the bonding interaction between the surface and water; (ii) a Gaussian term to improve the surface corrugation and (iii) two terms describing the angular dependence of the interaction energy. The 12 parameters of this force field are fitted against a set of 210 adsorption geometries of water on Pt(111). The performance of GAL17 is compared to several other approaches, that have not been validated against extensive first principles computations yet. Their respective accuracy is evaluated on an extended set of 802 adsorption geometries of $H_2O$ on Pt(111), 52 geometries derived from ice-like layers and an MD simulation of an interface between a c(4x6) Pt(111) surface and a water layer of 14 Å thickness. The newly developed GAL17 force field provides a significant improvement over previously existing force fields for Pt(111)/$H_2O$ interactions. Its well-balanced performance suggests that it is an ideal candidate to generate relevant geometries for the metal/water interface, paving the way to a representative sampling of the equilibrium distribution at the interface and to predict solvation free energies at the solid/liquid interface.

# 1 Introduction

In the last ten years, molecular modeling has matured to become a valuable tool during catalyst screening and development.[1–3] With the advent of biomass conversion, where water is almost omnipresent and for which metal catalysts are key for hydrogenations, reforming and many other transformations,[4,5] the demand for atomistic understanding of reactions at the aqueous/metal interface has soared. There are also many other important processes that occur at the metal/liquid interface, such as corrosion, electrochemistry, lubrification and biomedical applications as for example cancer phototherapy by gold nano-particles.[6,7] Experimentally and computationally it has been shown that, depending on the catalyst, water can play a non-innocent role during heterogeneous catalysis.[8–11] However, the computational approaches that are well suited to describe reactions at the solid-gas-phase interface are

not necessarily suitable to describe the solid-liquid interface: the amorphous character of these interfaces make static computations questionable, while *ab initio* molecular dynamics (AIMD) simulations are too costly to be routinely applied[12–16] and also the cost of adaptive QM/MM is prohibitive for metal surfaces.[17,18] Therefore, approximate methods have been developed aiming at representing the solid-liquid interface. Implicit solvent models, well established for molecular computations already in the 1990s,[19] have been developed lately for periodic systems[20–22] and made publicly available only very recently, first in VASP[23] and by now also in CP2K,[24] jDFTx.[25] and Quantum-Espresso[26]. However, the accuracy of these models remains largely unknown for metal/water interfaces.[27] Microsolvation, where a small number of crucial water molecules are included explicitly, has been applied since the pioneering work by Neurock and co-workers[28] to capture the direct effect of water on reaction pathways.[29,30] Hybrid methods, where the microsolvation is complemented by an implicit solvent are particularly attractive in terms of computational efficiency, but consistent treatment of the explicit water molecules remains a significant challenge.[9,31–34] Another approach is based on ice-like structures,[35–39] which are motivated by low-temperature surface science studies which have evidenced the existence of these arrangements over many transition metal surfaces.[40–42] However, these rigid networks are unlikely to be representative at ambient temperature and even less so at the elevated temperatures applied, for instance, in aqueous-phase reforming.[43] Reoptimizing structures obtained from short AIMD simulations is yet an other strategy,[8,44] but it remains unclear to which extent these basically arbitrarily selected water arrangements are representative of the properties at the solid-liquid interface.

While implicit solvation methods are, without any doubt, the most convenient and efficient ones for large-scale applications,[45,46] several approaches have been devised to replace the implicit solvent by an effective field (or solvation energy) obtained from molecular mechanics based molecular dynamics (MMMD) simulations or related methods.[47–51] In contrast to AIMD, the MMMD simulations can easily access the necessary time scales (ns range for equilibration) and length scales that are required to equilibrate these interfaces and to

avoid spurious effects due to 2D periodic repetitions of water configurations. Furthermore, these approaches allow, at least in principle, to assess also the subtle change in entropy upon adsorption, which, due to the competition between the solvent and the adsorbate for adsorption on the surface and the associated solvent reorganization at the interface, is far from trivial to assess.[52–54] Note, that already for reactions in solution, the situation is significantly more complicated than in the gas-phase, which explains the use of rough approximations in the literature, approximating solution phase entropy changes as half of the values obtained in the gas-phase.[55,56]

However, methods that rely on molecular mechanics introduce a different problem: the accuracy of the force field. The success of force fields for biological systems heavily relies on two pillars: First, there exist many experimentally resolved crystal or NMR solution structures which allow to validate a given force field. Second, the functional form has reached a certain consensus, with a clear distinction of bonded and non-bonded parameters describing bonds/angles, and long-range and short-range repulsive (Coulomb and Lennard-Jones) interactions, respectively. The problem of water/metal interfaces is that the experiments (in particular averaged information from X-ray scattering[57] or local information from spectroscopy[58,59] ) do not yield nearly enough information to (in-)validate any proposed force field. Therefore, the "constraints" from experiment are very few and largely insufficient to validate a given theoretical model. This might explain why the last 30 years have seen numerous and contradictory force fields and simulations for metal-water interfaces.[60–69] Furthermore, not even the functional form is obvious: Water adsorption on metals has often at least some degree of directional covalency, without creating well defined covalent bonds. The most successful recent water models have been parameterized against large data sets of high level correlated electronic structure computations.[70,71] Unfortunately, for the size and nature of metal/liquid interfaces, the highest achievable level for a sufficient number of distinct geometries is density functional theory (DFT) in the dispersion corrected generalized gradient approximation. Our level of theory (PBE-dDsC[72,73]) has been benchmarked against various experimental

adsorption energies from single-crystal microcalorimetry and found to perform very well.[74] As shown below, the preference of water to adsorb on top sites is also well reproduced. This level is significantly more reliable than the extended Huckel computations[75] used for some of the older (but still popular) parametrizations.[62,64] Amongst previous works, only the neural network model by Behler and co-workers[68] and the very recent work by Johnston and co-workers[69] have made extensive use of first principles computations for training and validation. However, as best illustrated by the repeated discussion on the "best suitable functional", the choice of the particular flavor remains debatable[14] and the sensitivity of the final result on this choice is, similar to the true structure of the water/metal interface, unknown.

Herein we propose a functional form for the metal-water interaction that is designed to capture the major effects, in particular the directional chemisorption interaction as well as the short-range repulsion and long-range attraction. Furthermore, in the interest of being able to combine the interaction potential with well established force fields for solutes, our functional form is rather simple (compared to a neural network), with few parameters that do not depend on the water model. Hence, our water-metal force field can be complemented with diverse water–water interaction potentials, thus assessing the sensitivity of the interface structuring on the competition between water–water and water–surface interaction, a question which has not been adressed frequently in the literature (see ref 76 for an exception). Our force field is implemented in the publicly available *sander* program, from the AmberTools package (available in version 18).[77] Furthermore, we introduce a training and validation set to assess the quality of a metal/water force field. On the one hand, we extensively sample the adsorption energy as a function of adsorption site (hollow, bridge and top), rotational angles and distance from the surface. On the other hand, we also try to reproduce the adsorption energy for (partial) ice-like layers. This benchmark data has also been used to assess previously proposed schemes, in particular the METAL force field by Heinz *et al.*[78] and the IC-QM/MM (and QM/MM) by Golze *et al.*[79] where the water–water interaction

is treated at the DFT level, while the water-surface interaction is given by the potential of Siepmann and Sprik,[79] which has been used extensively in MMMD studies.[66] The potential by Spohr and Heinzinger[61,62] has been among the first atomistic potentials trying to describe the interaction between water and a platinum surface. The Spohr-Heinzinger potential is an interesting contender among the Pt–$H_2O$ force fields, last but not least since it includes an explicit term for H – Pt interaction. Therefore, we herein also test this potential in its original form, although it has been parametrized for Pt(100). Finally, from MD simulations we demonstrate the sensitivity of the orientational preference of $H_2O$ at the interface not only to the water-metal interaction potential, but also to the water–water interaction. As a consequence, the time scale for equilibration of the interfacial water is around 0.5 ns in agreement with previous studies.[66,80] This is far beyond the scope of AIMD for an interface with a suitable size.

## 2 Functional Form of the Force Field

The functional form for the force field between water and metallic surfaces has been the subject of several previous publications, with a wide range of sophistication proposed: from simple Lennard-Jones potentials (like the METAL force field of Heinz *et al.*)[78] to the ReaxFF[81] or neural networks[68] for the case of copper surfaces. After extensive testing, we herein propose a pair-wise potential that is completely independent of the chosen model for the water – water interactions. This has the advantage that the effect of the water model on the interface structure can be assessed straight forwardly and, in the future, QM/MM simulations in analogy to what has been done for the Siepmann-Sprik potential[64,79] are in reach. Additionally, we have developed the functional form in view of a possible generalization to other molecules, in particular alcohols and polyols, which are important species in bio-mass processing.

A united atom like approach was chosen in which the water-Pt interaction depends on the distance between the water and the metallic surface, and on the orientation of the

water molecule with respect to the surface normal. The basic terms of our force field are a standard Lennard-Jones potential ($V_{\mathrm{LJ}}$) between the surface and the oxygen atom, which takes care of the long-range dispersion and the short-range repulsion. The surface corrugation is improved by a Gaussian potential ($V_{\mathrm{Gauss}}$). Since water and its interaction with a surface is not spherically symmetric, we also introduce two terms that improve the description of the angular dependence of the interaction energy ($V_{\mathrm{Ang}}$). This force field will thus be called GAL17.

$$V_{\mathrm{GAL17}}(\mathrm{Pt}, \mathrm{H_2O}) = V_{\mathrm{Gauss}} + V_{\mathrm{Ang}} + V_{\mathrm{LJ}}. \tag{1}$$

We have considered including electrostatic interactions via the image charge rod model.[82] However, we found that the corresponding contributions are comparatively small and therefore do not justify the significantly larger computational cost associated with the thermalization of the dipoles.[83,84] Hence we decided not to include an explicit image charge term. In agreement with previous reports[85–87] water–water interactions are significantly modified by the presence of the metal surface. This is likely to be a combination of charge-transfer and many-body polarization effects. Many-body terms between water molecules are,[88,89] just like the interactions between the platinum surface and more than one water molecule, beyond the scope of the current force field, which is neither polarizable nor based on fluctuating charges in order to keep the computational cost down and allow its implementation with minimal modification of classical MD codes. The following subsections detail the three terms of Eq. 1.

## 2.1 Chemisorption and Lennard-Jones Potential

A Lennard-Jones potential between the Pt and O atoms leads to a preferred adsorption of water on hollow sites (i.e., in the triangle between neighboring Pt atoms), while DFT computations[41] and experiments[90] unambiguously identify the adsorption site on top position as most stable. To correct this, Corni and co-workers have proposed to introduce LJ potentials

between water and "virtual sites" (VS) located at the hollow sites of the outermost metal layer. By simple geometry, these interactions reverse the situation, allowing to retrieve the preference for top adsorption.[65] However, the functional form of the Lennard-Jones potential does not allow to consistently reproduce the correct magnitude of the energy difference between top and hollow sites on platinum. Therefore, we herein introduce an anisotropic Gaussian function to correct the surface corrugation, i.e., the difference in adsorption energy between top and hollow sites. Such a potential might be reminiscent of the famous Morse potential or its modern extensions.[91]

The combination of Lennard-Jones and a Gaussian potential opens up two possibilities: Either, the Lennard-Jones potential is centered on the virtual sites to get the minimum at the top sites. In this case, the attraction at the VS is too strong, requiring a repulsive Gaussian centered on VS. Or, the Lennard-Jones potential can be based on Pt atoms, governing the attraction observed at the hollow sites. In this case, the Gaussian potential needs to be attractive and also centered at the Pt atoms in order to account for the stronger (chemisorption) interaction on top sites compared to the hollow sites. The first possibility is inspired by the work of Corni and co-workers and its results are discussed in the Supporting Information under the name vsGAL17. It suffices here to say that the results are quite similar to the second possibility, GAL17. We prefer to avoid the virtual sites, also because it allows us to give a physical meaning to the two terms of the following equation: physisorption and chemisorption for the first and second term, respectively.

$$V_{\mathrm{LJ}} + V_{\mathrm{Gauss}} = \sum_{i\in[\mathrm{O}]} \sum_{j\in[\mathrm{Pt}]} \varepsilon_{ij} \left[ \left( \frac{r_{\min}}{r_{ij}} \right)^{12} - 2 \left( \frac{r_{\min}}{r_{ij}} \right)^{6} \right] - \sum_{i\in[\mathrm{O}]} \sum_{j\in[\mathrm{Pt}]} \varepsilon_{\mathrm{att}} e^{-b_{\parallel}\left((x_j-x_i)^2+(y_j-y_i)^2\right)} e^{-b_{\perp}(z_j-z_i)^2} \quad (2)$$

where $r_{ij}$ is the distance between atoms $i$ and $j$; $\varepsilon_{ij}$ is the minimum of the LJ energy well which is located at $r_{\min}$. $\varepsilon_{\mathrm{att}}$ is the magnitude of the Gaussian attraction. The Gaussian

function itself is anisotropic in the out-of-plane direction (here assumed to be the $z$ axis), with the two in-plane directions $(x, y)$ being equivalent due to symmetry: $b_{\parallel}$ and $b_{\perp}$ are constants that define the width of the Gaussian in the surface plane and out-of-plane directions, respectively.

## 2.2 Angular correction

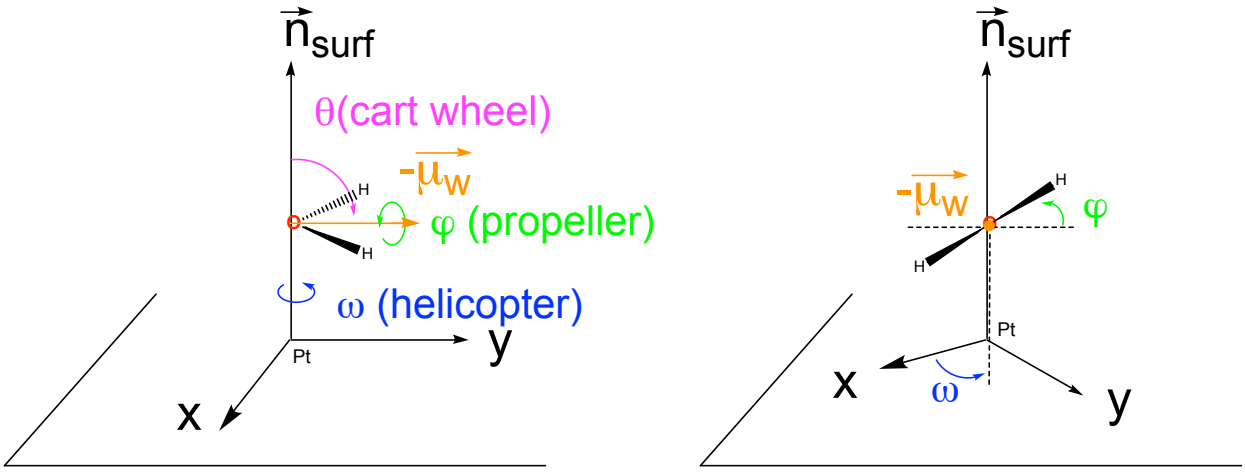


Figure 1: Definition of angles between a water molecule and a platinum surface in the x-y plane. $\vec{\mu}_w$ and $\vec{n}$ are the water dipole (i.e., the bisector of the H–O–H angle) and surface normal vectors, respectively.

According to our tests, two angles are key: the cart-wheel angle $\theta$ and the propeller angle $\varphi$, which are depicted in Figure 1. The helicopter motion $\omega$, has been found to lead to very small energy variations and is, therefore, not investigated in details. Fortunately for us, to a good approximation, the effect of the two angles are separable, avoiding complex expressions and making the functional form physically more transparent. In fact, it turns out that only the cart-wheel angle $\theta$, which describes the orientation of the dipole moment with respect to the surface normal, requires a potential that depends explicitly on this angle. It can be approximated as a truncated Fourier expansion, switched off smoothly at a certain distance away from the surface by multiplying with a Fermi function. The position of the surface is defined as the plane going through the topmost layer of Pt atoms. The latter are held fixed

in all our simulations. The $\varphi$ dependence is well reproduced by a repulsive term between the surface and the hydrogens, decaying as $1/r^5$, with the power five being adjusted empirically on DFT data.

In summary, for each water molecule the angular correction potential takes the form

$$V_{\text{ang}} = \left(1 - \frac{1}{e^{-s_{\text{ang}}(r_{\text{O,surf}}/r_{\text{ang}}-1)}+1}\right) \sum_{n=1}^{4} a_n \cos(n\theta) + \sum_{i=1}^{2} \frac{A_{\text{Hsurf}}}{r^5_{\text{H}_i,\text{surf}}} \tag{3}$$

where $r_{\text{O,surf}}$, $r_{\text{H}_1,\text{surf}}$, and $r_{\text{H}_2,\text{surf}}$ are the distances between the oxygen atom and the two hydrogen atoms, respectively, and the platinum surface, while $s_{\text{ang}}$ defines the steepness and $r_{\text{ang}}$ the location of the mid-point of the Fermi function. $a_n$ are the coefficients in the Fourier series, while $A_{\text{Hsurf}}$ is the repulsion parameter between the hydrogen atoms and the surface.

Given the above expressions, we have the following 12 parameters: two for the LJ potential ($\varepsilon_{ij}$, $r_{\text{min}}$) and three for the anisotropic Gaussian ($\varepsilon_{\text{rep/att}}$, $b_{\parallel}$, $b_{\perp}$) from Eq. 2.1, six for the distance dependent $\theta$ dependence ($s_{\text{ang}}$, $r_{\text{ang}}$, $a_n(n = [1, 4])$), and one for the repulsion between the hydrogen atoms and the surface ($A_{\text{Hsurf}}$) from Eq. 3.

# 3 Computational Details

## 3.1 DFT Computations

All static DFT computations have been carried out using VASP 5.4.1 [92,93] using periodic boundary conditions, the PBE[72] generalized gradient approximation (GGA) exchange-correlation functional with dDsC dispersion correction,[73,74] and an energy cutoff of 400 eV for the expansion of the plane-wave basis set. The electron–ion interactions are described by the PAW formalism.[94,95] We have constructed a series of 802 configurations of a single water molecule adsorbed on a p(3×3) Pt(111) unit cell with 4e metallic layers (Figure 2a). The Pt–Pt distance was optimized for the bulk and found to be 2.812 Å. The slabs are separated by a vacuum of 20 Å in order to minimize interactions between periodic images. The Brillouin

zone was sampled by a Γ-centered $3 \times 3 \times 1$ Monkhorst-Pack K-points grid. An idealized geometry (as cut from bulk Pt) was adopted for the metallic layers, while the water molecule was taken from a DFT optimization (O–H: 0.98 Å and a H–O–H angle of 105.32°). 13 values for $\theta$ were picked spaced by 30°, except for the "end points" which were taken to be 10° and 340°. These $\theta$ values were combined with $\varphi = 0$ and 12 distances (from 2.1 to 6.0 Å above the surface for the top site), leading to a set of 156 configurations. Similarly, 11 distances (2.3 to 6.0 Å) were selected to assess the same set of orientations above the bridge and hcp site, summing up to 286 configurations. To study the $\varphi$ dependence, 10 values between 20° and 180° were selected and combined with 3 values for $\theta$ (30, 90 and 120°) at the same 12 distances above the top site generating 360 configurations.

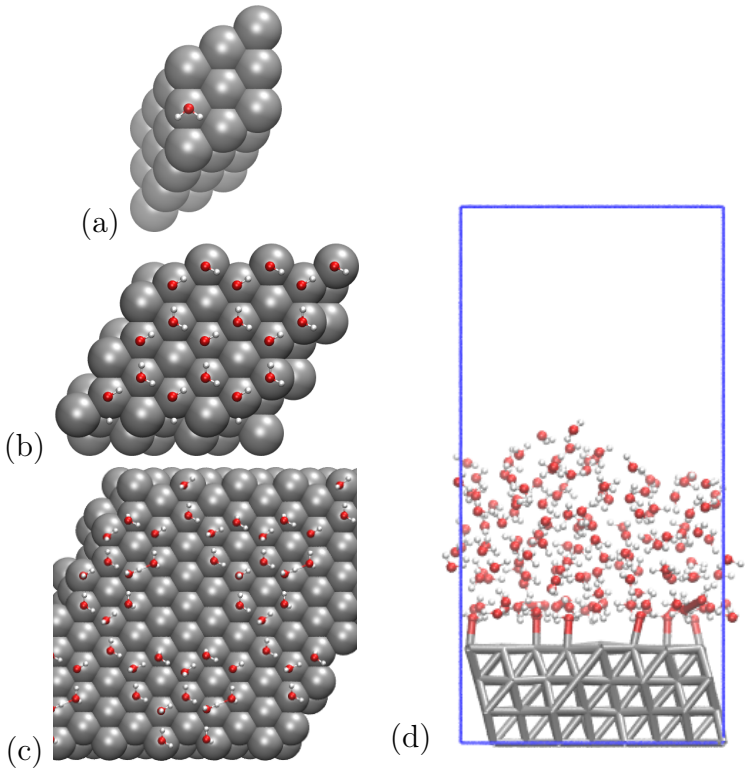


Figure 2: Systems used in this study. Fitting set: (a) One configuration of a single molecule adsorbed on the Pt(111) surface; Validation sets: (b) Full Ice layer used, (c) Defective ice layer, (d) Snapshot of the MD simulation.The blue frame corresponds to the unit cell. The water thickness is approximatively 14 Å.

We also built two validation sets: the first one is based on the two main structures

proposed for an ice-like layer on Pt(111): $H_{up}$ and $H_{down}$, which are both hexagonal structures. In this structure, water molecules are alternating between a "flat" chemisorption mode and water molecules that are H-bonded to the chemisorbed water molecules, with the second hydrogen molecule either pointing up or down. All these geometries are fully optimized at the DFT level on a 3 layer Pt(111) (18 water molecules on a $3\sqrt{3} \times 3\sqrt{3}$R30° unit cell), for which the Brillouin zone was sampled by a Γ-centered $3 \times 3 \times 1$ Monkhorst-Pack K-point grid. From the two full ice-like layers (Figure 2b), 52 configurations were constructed and optimized by removing one to six molecules (Figure 2c) or by keeping only one to six molecules. The DFT optimization induced significant re-organizations in several instances. Therefore, this validation set will be discussed as a whole, without distinguishing between $H_{up}$ and $H_{down}$ derived structures.

For the second set, we have performed extensive *ab initio* molecular dynamics simulations on a c$(4 \times 6)$ unit cell of four metallic layers with 151 water molecules on top of it (Figure 2d). This leads to a water layer of approximately 14 Å on top of the surface. This thickness is sufficient to recover bulk water above the surface.[12] All these MD simulations were performed with CP2K[24] and the Brillouin zone was probed at the Γ point only. The initial configuration was provided by D. Golze and corresponds to the equilibrated IC-QM/MM simulation presented in ref 79. The Pt layer was, however, re-optimized at the PBE-D3[72,96] level since the molecular mechanics generated structure corresponds to a (hot) configuration far from equilibrium at the DFT level. After this preparatory adjustment for the change of the level of theory, the system was subjected to 10 ps of Born-Oppenheimer molecular dynamics using a 1 fs timestep, while simulating protons as deuterium at 300 K and keeping the bottom two layers of Pt frozen. The wave function was expanded in a polarized double zeta basis set and the charge density computed on a grid characterized by a 400 au cutoff. The wave function was converged to $10^{-6}$ au, applying a Fermi smearing of 300 K and diagonalizing the Kohn-Sham Hamiltonian.

## 3.2 MM Computations

All MM computations were performed with a locally modified version of *sander* of the AmberTools simulation package.[77] The GAL17 implementation is publicly available in AmberTools 18. Except for the MD simulation of the $Pt/H_2O$ interface, all MM computations were single point energies. The non-bonded cutoff distance was set to 8 Å, which required to set the safety distance parameter (skinnb) to 0.4 Å due to the size of the unit cell for the $Pt/H_2O$ interface. For all other computations we simply replicated the original DFT unit cell by four in each in-plane direction and divided the resulting adsorption energy by sixteen. Standard settings were used for the particle mesh Ewald treatment of the long-range electrostatics.[97] During MD simulations, the surface atoms were held fixed at their initial position by applying "belly" dynamics, i.e., zeroing out their velocities at each time step. The temperature was maintained at 298.15 K through the weak coupling thermostat by Berendsen[98] and the water models were held rigid with a tolerance of $10^{-7}$ Å applying the default algorithms in AMBER.[99] For the 10 ps simulations, a time step of 1 fs was used, while longer simulation were performed with a 2 fs time step.

## 3.3 IC-QM/MM Computations

All (IC-)QM/MM computations were perfomed with CP2K, v 4.0. A typical input, is provided in the supporting information. In these simulations, the water-water interaction is modelled at the PBE-D3[72,96] level, while the metallic surface is described by EAM and the water-surface interaction is accounted for by the Siepmann-Sprik potential with or without including the image charge (IC) effect. All other technical settings were equivalent to the ones used for the ab initio MD simulations mentioned above, except that the highly efficient orbital transformation[100] was applied for the wave function optimization instead of the diagonalization and that all Pt atoms were kept fixed during the simulation. For the single point computations on the p(3×3) unit cell, it was necessary to double the in plane repetitions, similar to the AMBER simulations, in order to properly account for the atoms within the

cutoff distance of 8 Å.

## 3.4 Fitting of the Parameters

The parameters of our force field could have been determined in a force matching scheme to the DFT MD simulations.[101] However, such a strategy would make the fit specific to a given water model. Furthermore, the discrepancy in water–water description between DFT and a given force field is likely to skew the fit for the $H_2O$–Pt interaction. Therefore, we prefer to optimize the parameters only on the training set described below. This optimization was achieved through a Nelder-Mead "amoeba/simplex" algorithm as implemented by A. Garcia and distributed within the SIESTA simulation package,[102] targeting a minimal root mean square deviation (RMSD) over the training set.

Of the 802 water orientations, only 210 configurations were used as a training set. In particular, the 22 adsorptions for $\theta = 90°$, $\varphi = 0°$ above the hcp and bridge site were included, as well as the $\theta$ dependence on the top site for the 8 smallest distances. The $\varphi$ dependence was probed for the 4 smallest distances. However, configurations leading to adsorption energies above 1 eV (23 kcal $mol^{-1}$) have been excluded, leading to 210 instead of the "full" 246 configurations.

The functional form of our force field is rather general and should, therefore, be suitable for various metals, from surfaces that interact strongly, e.g., Ru(0001), or weakly, e.g., Au(111) with water molecules. The parameters determined for Pt(111) are unlikely to be transferable to these materials: we expect them to depend on the radius of the metal atoms and on the oxophilic character of the metal. However, with the protocol established, other metal surfaces can be parametrized at a relatively low complexity. These extensions are currently underway.

Table 1: Optimized parameters and root mean square deviation (RMSD) for the GAL17 force field. The superscript "tot", "validation" and "bound" refer to the full set of 802 configurations, the 592 configurations outside the training set and the 700 configurations with negative adsorption energies, respectively.

| Parameter | GAL17 | Units |
|---|---|---|
| $\varepsilon_{ij}$ | 6.410 | kcal mol$^{-1}$ |
| $r_{\min}$ | 1.136 | Å |
| $\varepsilon_{\text{att}}$ | -8.901 | kcal mol$^{-1}$ |
| $b_{\parallel}$ | 9.331 | Å$^{-2}$ |
| $b_{\perp}$ | 0.102 | Å$^{-2}$ |
| $s_{\text{ang}}$ | 11.135 | |
| $r_{\text{ang}}$ | 2.441 | Å |
| $a_1$ | 15.768 | kcal mol$^{-1}$ |
| $a_2$ | 1.594 | kcal mol$^{-1}$ |
| $a_3$ | 1.922 | kcal mol$^{-1}$ |
| $a_4$ | 2.838 | kcal mol$^{-1}$ |
| $A_{\text{Hsurf}}$ | 304.081 | kcal mol$^{-1}$Å$^5$ |
| RMSD$^{\text{tot}}$ | 2.44 | kcal mol$^{-1}$ |
| RMSD$^{\text{validation}}$ | 2.68 | kcal mol$^{-1}$ |
| RMSD$^{\text{bound}}$ | 1.67 | kcal mol$^{-1}$ |

# 4 Results and Discussion

## 4.1 Water Adsorption and Rotation

The 12 characteristic parameters of our force field have been fitted to minimize the RMSD and are given in Table 1. As a first test, we present the adsorption energies of all 802 adsorption energies of a single water molecule on a p(3×3) Pt(111) surface. Figure 3 shows the correlation for the full set of 802 adsorption energies. Since GAL17 has been trained on 210 configurations, Figure S1 shows the corresponding graph for the validation set (592 configurations) and Table 1 gives the RMSD for the full and the validation set. Both Figures convey the same conclusions, but Figure 3 shows also the low lying and thus most important configurations. We conclude that GAL17 correlates quite well with the DFT data, which is also reflected in the relatively small RMSD over the entire set of 2.44 kcal mol$^{-1}$. As can be expected, restricting the RMSD computation to the 592 configuration outside of the training set leads to a small increase. However, with 2.68 kcal mol$^{-1}$, GAL17 still performs very

well. Furthermore, if we consider only the geometries in which the water molecule is bound (negative adsorption energy), the RMSD drops to 1.67 kcal mol$^{-1}$. Focusing on the region of negative adsorption energies (right pannel), we see that GAL17 tends to underestimate the stability of configurations which have a DFT adsorption energy of -5 to -2 kcal mol$^{-1}$. While GAL17 is clearly not perfect, the comparison with the other force fields shows a significant improvement, be it the seminal force field of Spohr and Heinzinger (also known as Spohr potential)[61,62] or compared to "state of the art" methods, i.e., the Siepmann-Sprik potential[64] coupled to a DFT description for water with or without image charge effects ((IC-)QM/MM)[79] or the much simpler, but popular, Lennard-Jones only potential called METAL by Heinz *et al.*[78] The most characteristic difference between our force field and these predecessors are the "horizontal lines" observed for the latter: for these series of configurations, the force field do not show any significant variation in the adsorption energy, while DFT assigns energy differences up to 150 kcal mol$^{-1}$. The second immediate observation is that the METAL force field binds water molecules rather weakly. A more detailed analysis (see Figure 6) shows that the interaction on top is too weak, while hollow sites are overstabilized. Indeed, when comparing the simple pair-wise attractive/repulsive term of the three different force fields, we find that the METAL force field is not very attractive (see SI).

Investigating the origin of the "horizontal lines" observed in Figure 3 for the force fields from the literature, the $\varphi$ dependence is quickly identified as the culprit: Figure 4 illustrates the energy evolution as a function of $\varphi$ at an oxygen position of 2.6 Å above a Pt atom and a value of 90° for $\theta$. Along this rotation around the dipole moment of the molecule, the hydrogen atoms get closer to the surface, effectively "bumping" into it, leading to an increase of up to 14 kcal mol$^{-1}$ according to DFT. This increase is quite faithfully reproduced by the $r^{-5}$ repulsion included in our force field, but is totally absent in most of the force fields of the literature (Figure 4). The exception is the Spohr potential, which successfully includes a Pt–H repulsive term that improves the $\varphi$ dependence. However, this repulsion is too weak compared to the DFT results, demonstrating the need for a more balanced description and

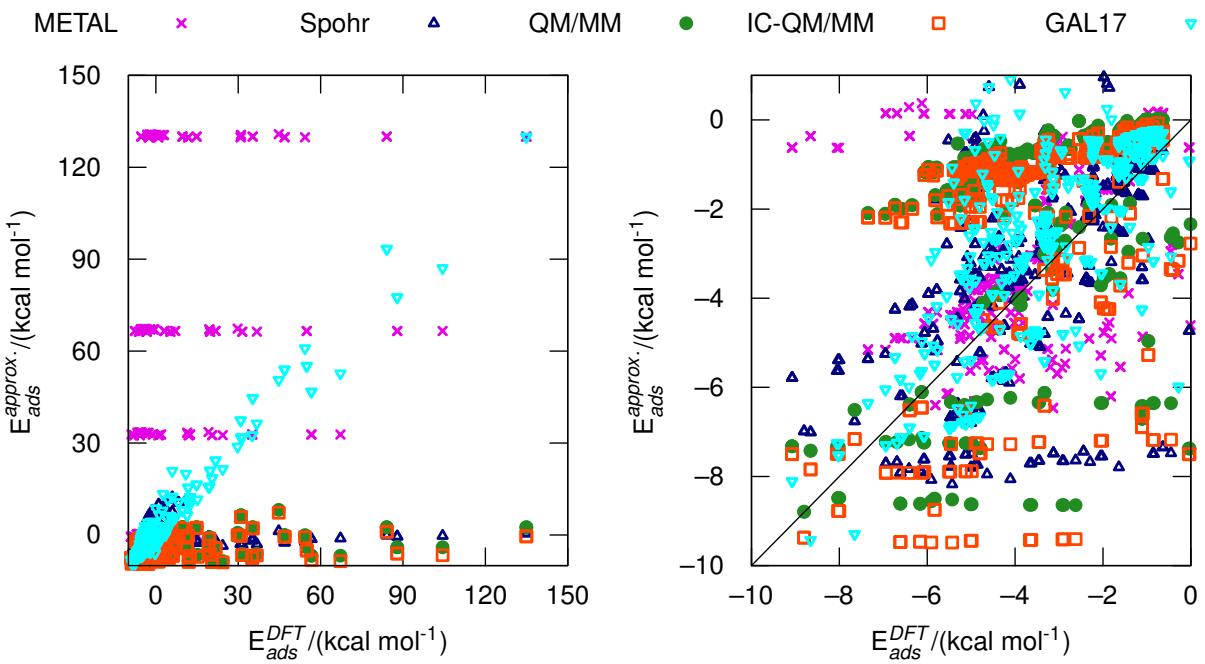


Figure 3: Correlation between DFT data and various approximate methods for the adsorption of a water molecule on a p(3x3) unit cell for various adsorption sites and combinations of $\theta$ and $\phi$. Left: overall correlation, right: Correlation for geometries with negative DFT adsorption energies.

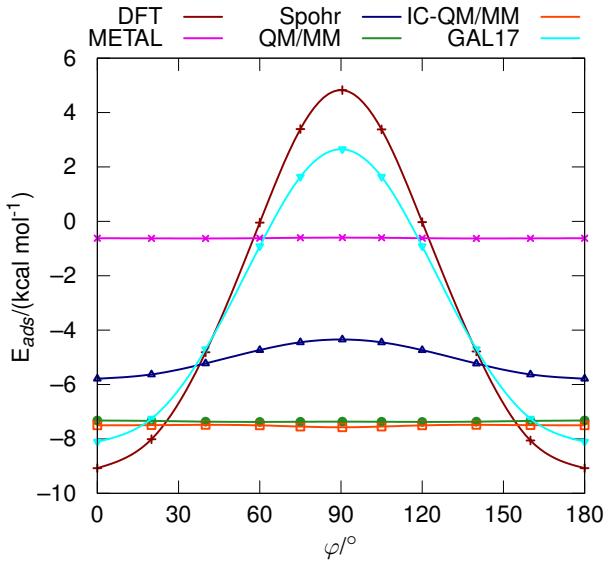


Figure 4: Adsorption of a water molecule on a p(3x3) unit cell on a top site (2.6 Å above a Pt atom), as a function of $\varphi$, the angle between the dipole moment and the out-of-plane axis at $\theta = 90$, computed with various methods.

careful parametrization. This strongly suggests that our force field is likely to sample a more relevant configurational space than previous approaches, which is particularly important in QM/MM re-sampling approaches, where configurations are extracted from MM simulations and their energies re-weighted at the QM level.[103,104]

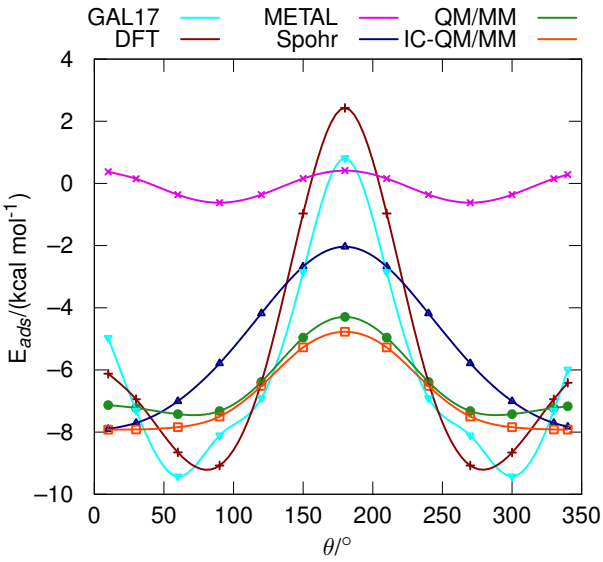


Figure 5: Adsorption of a water molecule on a p(3x3) unit cell on a top site (2.6 Å above a Pt atom), as a function of $\theta$, the angle between the dipole moment and the out-of-plane axis at $\varphi = 0$ computed with various methods.

Next, we turn to the rotation of the dipole moment with respect to the surface normal ($\theta$). At 90° the water molecule is parallel to the platinum surface (for $\varphi = 0$) and the lowest interaction energy is obtained (see Figure 5). Rotating it to 0° moves the hydrogen atoms up, which is associated with a loss of roughly 3 kcal mol$^{-1}$ according to DFT. Rotating in the other direction is strongly disfavored (+12 kcal mol$^{-1}$), since the hydrogen atoms get too close to the surface. These variations are well reproduced by the GAL17 force field. As can be expected, the METAL force field, where hydrogens are just described by point charges, cannot resolve this $\theta$ dependence either. The small variation observed in Figure 5 is electrostatic in nature and comes from the finite coverage used in these computations. The potential of Spohr and Heinzinger predicts a reasonable maximum around 180°, but it fails to identify 90° as the minimum. The force field of Siepmann and Sprik, on the other hand, depends

explicitly on $\theta$. Indeed, the variation has roughly the right shape for QM/MM although the magnitude of the differences is underestimated by more than a factor of two, which is most likely due to the outdated benchmark data used twenty years ago. When accounting for the image charge effect, however, the curve gets less satisfying, with a flat potential energy for angles between 0 and 90°(and, by symmetry, 270 and 360°).

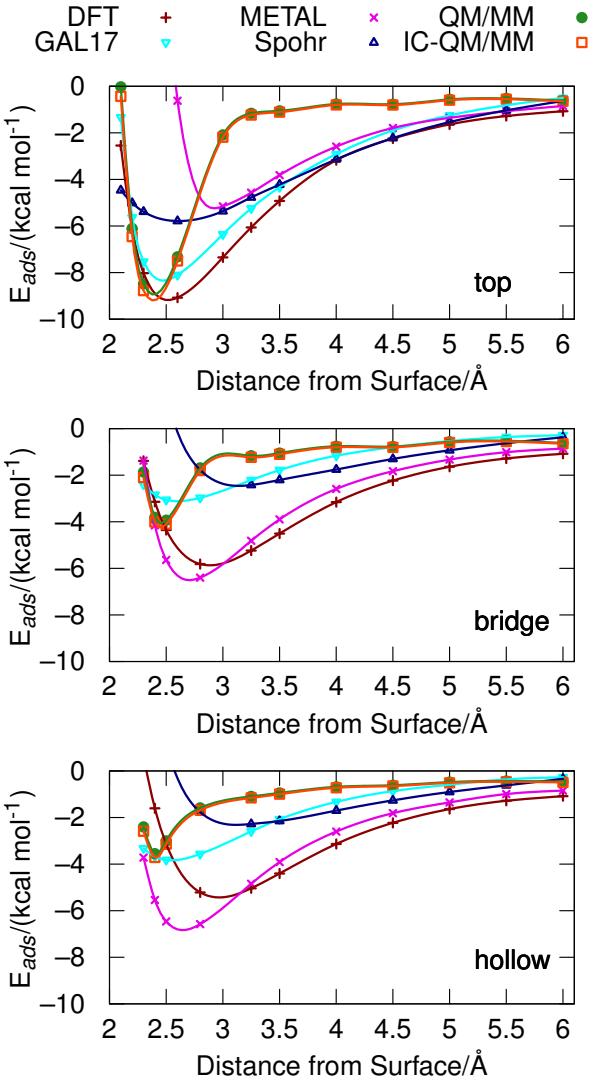


Figure 6: Adsorption of a water molecule on a p(3x3) unit cell on top (top), bridge (middle) and hollow (bottom) sites with $\theta = 90°$ and $\varphi = 0°$.

Finally, we assess the interaction energy as a function of the water-surface distance for a water molecule adsorbed with its molecular plane parallel to the surface plane at three different sites: top, bridge sites and hollow sites in Figure 6. At the DFT level, the top

adsorption is clearly preferred by at least 3 kcal mol$^{-1}$ with respect to the adsorption on a bridge site, which is only slightly more stable than the adsorption on the hollow site. Interestingly, at distance above 3.5 Å, the difference between the sites is disappearing quickly, which we see as a strong indication that the top site is stabilized by chemisorption, while the adsorption on bridge and hollow sites are due to physisorption. Regarding our force field, the agreement with DFT data is reasonable, although GAL17 underestimates the stability of the hollow and bridge sites. Also the difference in adsorption height for the minimum energy of the three sites (2.6 Å on top, but roughly 2.8 Å on bridge and hollow sites) is washed out. METAL, a pure LJ potential, predicts the hollow site to be most stable, while the top site is least stable, with an error of 4 kcal mol$^{-1}$ at the minimum energy positions. This is qualitatively wrong, since all DFT data indicates that the minimum should be at the top site, not the hollow site. Unfortunately, no pairwise, atom-centered potential is able to reproduce this preference, as also shown by Berg *et al.*[69] Note, however, that the long-range, physisorption, potential is quite well reproduced by the LJ potential, indicating that only the chemisorption energy is missing. The Spohr and Heinzinger potential accurately reproduces the site preference, but the interaction profile is too shallow compared to the reference DFT potential. The potential of Siepmann and Sprik is quite different. In this case, the use of a small training set with old, inaccurate benchmark data[75] is most likely to be at the origin of the issue: the long range part is severely underestimated (see also Figure S2 in the SI) and the minimum at the hollow and bridge sites is very narrow. The minimum at the top site, on the other hand, is quite well reproduced.

In summary, the analysis of 800 adsorption geometries of a water molecule on a p(3×3) unit cell has highlighted the challenges of capturing the orientational preferences of a water molecule over a platinum surface. In particular, the introduction of a repulsion between the surface and the hydrogen atoms was key for the rotation around the axis of the dipole moment, a term that is missing in most of the tested force fields from the literature, although it was present in some of the older parametrizations,[63,105] including the one by Spohr and Heinzinger

tested herein.[61] Additionally, reproducing the position and depth of the minima at top, bridge and hollow positions turned out to be less than trivial. Despite these small shortcomings, our force field still shows the best correlation against the reference data, capturing the essential physics of the orientation dependent adsorption energy of water on Pt(111), including a non-negligible contribution from chemisorption, which is notoriously difficult to be captured at the force field level.[106]

## 4.2 Water Aggregates: From Monomer to an Ice-Layer

Having established a reasonable accuracy for the interaction between a single water molecule and a platinum surface, the question is to which extent the potential is transferable to configurations with more than one water molecule. To this purpose, we have constructed a validation set based on ice-like layers on Pt(111) (see Computational Details).

Assessing structures with water–water and water–surface interactions also requires to choose a water model. Since the developed force field is completely independent of the water model, we decided to test several models, i.e., the TIPxP family with x=3,4 and 5,[107–109] the popular SPC/E[110] and the recent OPC model.[111] All of these models use a fixed water geometry and are non-polarizable. As for the reference of the water molecule, we consider that the least biased choice is an isolated water molecule. Hence, the -280 kcal mol$^{-1}$ adsorption energy for 18 water molecules (in a full $H_{down}$ layer) at the DFT level corresponds to an average adsorption/interaction energy of 15 kcal mol$^{-1}$, compared to the 9 kcal mol$^{-1}$ at the DFT minimum for a single water molecule, stressing the importance of the interaction between water molecules, including many-body effects,[88,89] which are not explicitly included in the pair-wise additive force fields tested here.

Figure 7 presents the correlation between the DFT data and the force field predictions of GAL17 combined with the five different water models, while Table 2 provides statistical measures for this set. The graph on the right shows the same data for the QM/MM and IC-QM/MM approaches, in which the many-body effects within the water layer are described

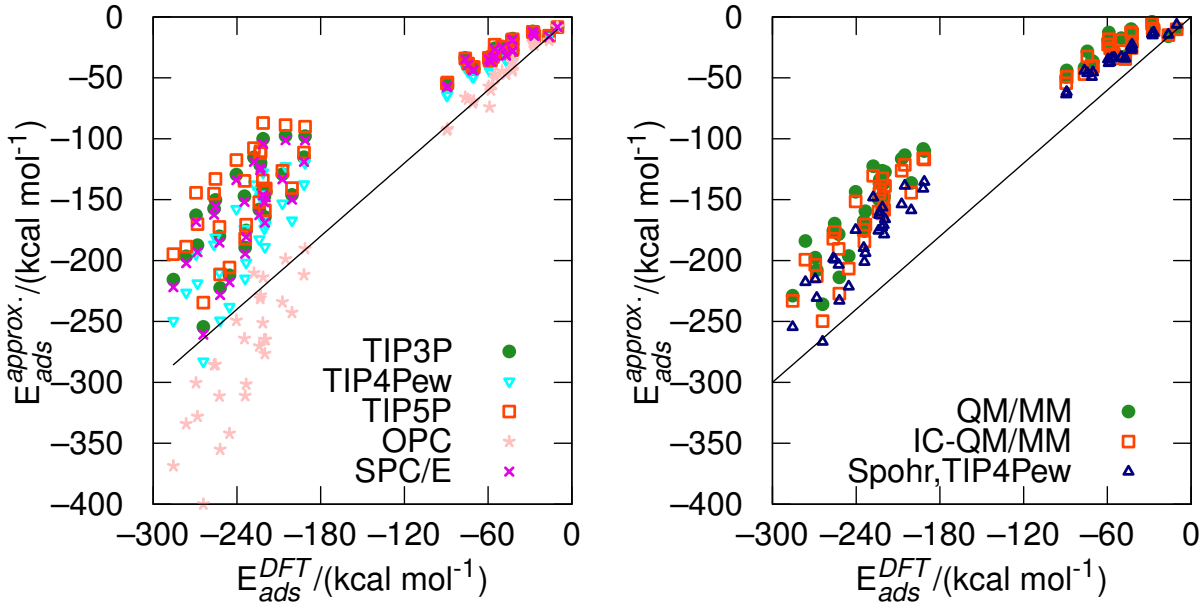


Figure 7: Correlation between DFT data and approximate methods for the adsorption energy of (defective) ice-like layers. Left: GAL17 using various water models. Right: IC-QM/MM and QM/MM using DFT for water–water interactions (from ref 79) and the Spohr-Heinzinger potential with the TIP4Pew water model.

at the DFT level, while the ones with the platinum surface are still not captured. Note that the METAL force field of Heinz and co-workers has been excluded in this Figure since the adsorption energies are very repulsive due to the use of DFT geometries and the shift to longer Pt-O distances of the minimum around the top sites evidenced in Figure 6.

The first observation is that the OPC water model is quite different compared to the other water models, overestimating the water-water interactions significantly. The other four water models yield rather similar results, with $R^2$ of 0.89 to 0.96. While the RMSD is lowest for OPC (3kcal mol$^{-1}$ per $H_2O$ or 40 kcal mol$^{-1}$ per system), it is TIP4Pew that fares overall best, with an RMSD of only 1 and 4 kcal mol$^{-1}$ larger (per $H_2O$ and per system, respectively), but with the smallest maximum error per system (94 kcal mol$^{-1}$, compared to 136 kcal mol$^{-1}$ for OPC) and the slope of the linear regression that is closest to 1.0. On the other hand, TIP5P is clearly the worst performer, with an $RMSD^{tot}$ of 70 kcal mol$^{-1}$, a maximum error of 143 kcal mol$^{-1}$ and a slope of only 0.66. With an error of 4 kcal mol$^{-1}$ per water molecule (for an interaction of about 15 kcal mol$^{-1}$) our approach is short from reaching the 5% accuracy

Table 2: Statistical measures for the accuracy of the description of (defective) ice-like layers. The root mean square deviation is reported per molecule $RMSD^{mol}$ and for the full system $RMSD^{tot}$.

| Method | $RMSD^{mol}$/ kcal mol$^{-1}$ | $RMSD^{tot}$/ kcal mol$^{-1}$ | Max. Error/ kcal mol$^{-1}$ | $R^2$ | Slope Slope | Intercept/ kcal mol$^{-1}$ |
|---|---|---|---|---|---|---|
| GAL17-TIP3P | 6 | 63 | 121 | 0.90 | 0.71 | 9 |
| GAL17-TIP4Pew | 4 | 44 | 94 | 0.93 | 0.83 | 10 |
| GAL17-TIP5P | 6 | 70 | 143 | 0.89 | 0.66 | 6 |
| GAL17-OPC | 3 | 40 | 136 | 0.96 | 1.25 | 16 |
| GAL17-SPC/E | 6 | 60 | 117 | 0.91 | 0.73 | 9 |
| Spohr-TIP4Pew | 3 | 23 | 58 | 0.98 | 0.97 | 14 |
| QM/MM | 7 | 61 | 105 | 0.95 | 0.76 | 17 |
| IC-QM/MM | 6 | 54 | 97 | 0.95 | 0.79 | 16 |

obtained by an empirical scheme for the adsorption energy of ice-like structures.[39] However, this approach contains explicit parameters for the strength of hydrogen bonds and the extra stabilization energy in a two dimensional ice-layer. Remarkably, for nearly complete ice-layers, all models predict two distinct families of structures, one being more strongly bound than the other for the same DFT interaction. Since the same applies to the QM/MM and IC-QM/MM simulations, we suggest that it is due to (many-body) charge transfer effects between the ice-like layer and the surface, which happen to be more pronounced in the $H_{down}$ than the $H_{up}$ conformations.

Given the approximations involved in the force field, the overall performance (error of $\sim$ 4 kcal mol$^{-1}$ per $H_2O$) for the defective water layers and water clusters on Pt(111) is rather encouraging. This validation set is also well described (albeit at higher computational cost) by the potential of Siepmann and Sprik in combination with a DFT treatment for the water–water interaction. This is partially due to the fact that the water molecules are all located close to the surface where the chemisorption potential is still active and not in the zone beyond 3.0 Å where the interaction is, erroneously, very weak (see Figure 6). By comparing the results for IC-QM/MM with QM/MM, we conclude that the image charge effect, which slightly improves the statistical measures (see Table 2) remains rather small, even for these more complex systems. This further confirms our choice of neglecting this

effect in GAL17. Somewhat surprisingly, the Spohr and Heinzinger potential in combination with TIP4Pew consistently outperforms all the other methods for this set.

In summary, water clusters and layers on Pt(111) are challenging test cases for pair-wise additive force fields. The combination of our force field with TIP4Pew seems to be a reasonably accurate option, rivaling the more expensive QM/MM methods, while being more accurate for non-equilibrium configurations and the longer-range surface–water interaction (*vide supra*).

## 4.3 Pt(111)/Water Interface

Characterizing the liquid/solid interface can be seen as the holy grail for interfacial sciences from lubricants and corrosion inhibition to catalysts and batteries, up to nanoparticles in biomedical contexts.[6,7,42]

Several characteristics have been proposed to describe the metal/liquid interface, with density profiles and histograms of characteristic angles being most popular. Therefore, we herein also present results for these quantities, in addition to the ratio of molecules that are on top of a Pt atom. Here, following our previous work on the recognition of adsorption modes on graphical lattices,[112] we define top, bridge and hollow sites as non-overlapping circles with a radius of 0.4 Å, covering roughly 37 % of the entire surface. Due to symmetry, the ratio top:bridge:hollow is 1:2:2. Hence, for a random distribution we expect 20% of the water molecules assigned to top sites.

Our best estimates come from 10 ps of AIMD for a 192 Pt atoms system with 151 water molecules on top of it, followed by a sufficient empty space to avoid confinement effects[12] at the cost of a liquid/vacuum interface. The interface was pre-equilibrated at the IC-QM/MM level of theory as explained in the Computational Details. The AIMD simulations are computationally extremely demanding: a single time step took, on average, 520 s (on 96 CPU cores), totaling to about 140'000 CPU core hours (or 60 days real time) for the 10 ps trajectory. To produce a fair comparison with the the force field methods, the same

simulation time has been applied, starting from the same initial configuration, except that the water molecules have been moved away from the surface by 1 Å for the setup using the METAL force field by Heinz in order to avoid the extremely repulsive distances with this force field when starting from DFT geometries. If not stated explicitly, the METAL force field is combined with the SPC/E water model as originally proposed,[78] while the Spohr-Heinzinger and GAL17 force field rely on the TIP4Pew model, since it gave the best agreement for the ice-like water layers (vide supra). The IC-QM/MM simulations can be considered to be better converged, since at least the initial structure is obtained from equilibrating at this level. However, it is not given that accumulating statistics of 10 ps is sufficient even for equilibration. Note that the IC-QM/MM simulations are around fifty times more efficient than pure AIMD, requiring approximately 60 s per time step on 16 CPU cores or roughly 2'600 CPU core hours for a 10 ps trajectory. Since the force field computations are again 4-5 orders of magnitude faster (15 ms per timestep on a single CPU core or 2.5 minutes for 10 ps), we were easily able to assess the equilibration time which turned out to be on the order of 100 ps, with trajectories of 500 ps generally providing converged statistics (see SI, Figure S4).

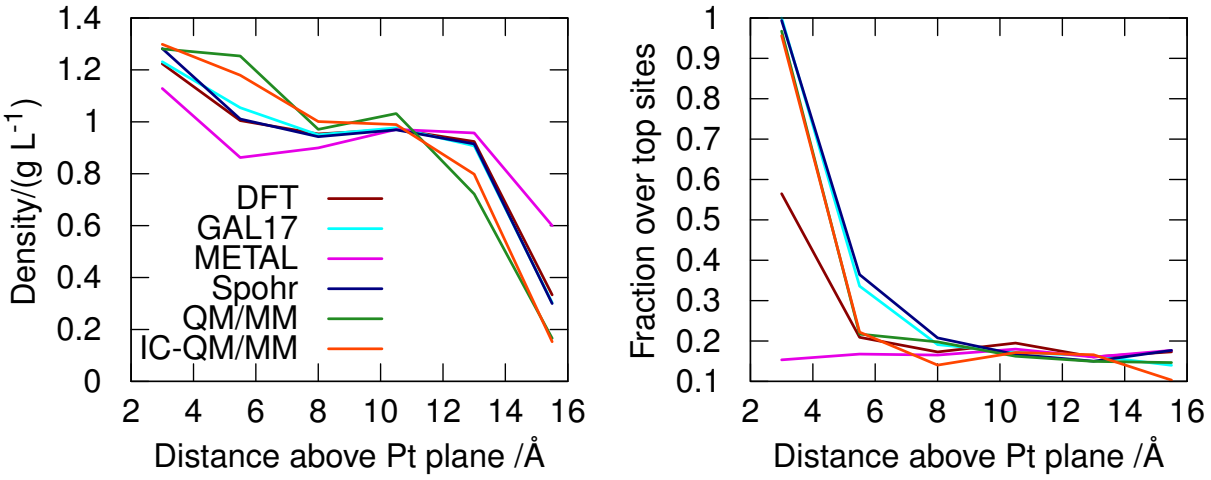


Figure 8: Density (left) and fraction of water molecules on top sites (right) as a function of the surface-solution distance for various methods as obtained from a 10 ps MD simultaion.

Having these limitations in mind, we can now discuss the results obtained from the 10 ps

of simulations for each method. Figure 8 presents the density as a function of the distance from the platinum nuclear plane. Generally, the density at the interface is 20-30% higher than in the bulk, which can be traced back to the significant chemisorption energy and is in qualitative agreement with experimental results for an electrified $Ag/H_2O$ interface.[57] The density in the bulk region (which here is found to start roughly 8 Å above the surface) corresponds to the expected 1 g $L^{-1}$ and is followed by the liquid/vapour (or vacuum) interface. Overall, we find that our water layer is probably somewhat slightly too thin, i.e., that the region that is affected by neither of the interfaces is small to non-existent, as evidenced by the single point around 10 Å for which all force fields roughly agree. Hence, we suggest that future investigations should have at least 20 Å of solvent on top of the platinum surface. Since running reliable isobaric simulations for these kind of systems is out of reach for any QM based method today, we do not recommend to use "filled" unit cells, i.e., two solid/liquid interfaces in order to avoid artifacts due to confinement effects.[12]

The right hand side of Figure 8 measures the in-plane ordering of the water layers. In agreement with previous reports, the potential by Siepmann and Sprik used in QM/MM and IC-QM/MM pushes all water molecules on top sites in the first hydration layer, so that hollow and bridge sites are not occupied at all. The same observation applies to the simulations based on the potential by Spohr and Heinzinger. The 10 ps of simulations at the AIMD level were sufficient to reduce the percentage of water on top positions to roughly 0.6. Hence, the bridge and hollow sites become also important at the DFT level, suggesting a less ordered interface than predicted previously.[66] Regarding the GAL17 force field, which underestimates the stability of bridge and hollow adsorption sites (see Figure 6), the ordering extends to the second layer of water molecules (see SI for vsGAL17 results, in which this problem is absent, because the bridge and hollow sites are overly stabilized). The METAL force field, on the other hand, is incapable of reproducing the expected ordering, lowering the ratio of top sites below 0.2, the ratio characteristic for a random distribution. This, again, could have been predicted simply by looking at Figure 6, where the hollow and bridge sites are most stable

for this force field.

In order to have a more detailed appreciation of the ordering at the first water layer over Pt(111) and how it varies with the different methods, Figure S7 represents typical structures. In all simulations, a significant degree of disordering is observed, although various sizes of ring-structures can be recognized. Compared to DFT, the force fields predict somewhat more ordered interfaces with a tendency of mixing six and four membered rings, rather than the five and six membered rings that dominate the DFT interface. This strongly suggests that these various motives, which can also be found in ice,[113] would need to be included in a force field fit that aims at a balanced description of water–water and water–metal interactions at the interface due to the inclusion of many-body effects.

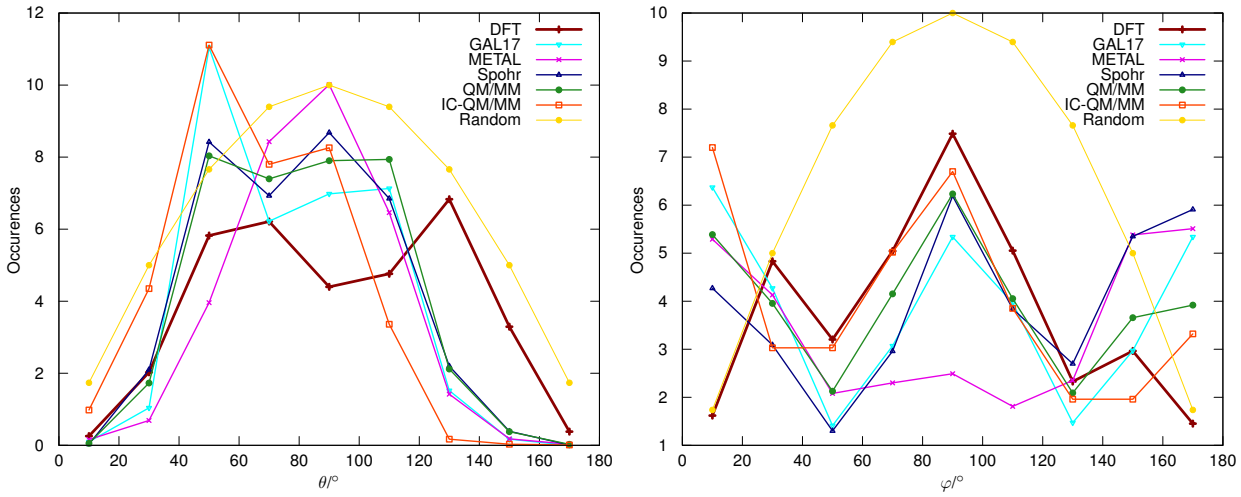


Figure 9: Distributions of $\theta$ (left) and $\varphi$ (right) for the first solvation layer for various methods as obtained from a 10 ps MD simultaion.

Having seen that 10 ps is sufficient to modify the site preference significantly and in agreement with the predictions for a single water molecule, we now investigate the angular preference within the first hydration layer in Figure 9 (for the corresponding results for the "bulk-like" layer around 8 Å, see Figure S6 in the SI). When compared to the random distributions, both angles ($\theta$, the orientation of the dipole moment with respect to the surface normal and $\varphi$, the angle describing the rotation of the water molecular plane around the dipole moment) show clear preferences. Regarding the nature of the preference, the different models

agree that having the water dipole perpendicular to the surface ($\theta \approx 0$ or 180°) is unfavorable. Where the models disagree, is regarding the question if inclining the dipole moment up (60°, GAL17 and IC-QM/MM) or down (120°, DFT) is energetically preferable compared to the "flat" (90°, METAL) adsorption mode. Both the QM/MM and the Spohr-Heinzinger potential predict a degeneracy of the "up" and "flat" lying dipole moments. Note, that this is the first time within this paper that we can evidence a significant difference between QM/MM and IC-QM/MM. While this is analogous to the findings of Tarmyshov *et al.* for isopropanol/water mixtures at the Pt(111) interface,[114] we can not exclude an artifact due to non-converged configurational sampling: Extending the GAL17 simulations to 500 ps, the interval between 60 and 120 becomes very flat (see Figure S4 in the SI). The situation is even worse for $\varphi$, where the convergence issues with respect to the sampling are enhanced. To conclude, there is no agreement between the methods regarding the balance between $\varphi = 90°$ and $\varphi = 0°$: depending on the method, $\varphi = 90°$ is a dominant maximum (DFT and random distribution) or a maximum that is almost degenerate with $\varphi = 0°$ (all other methods, except METAL). At first sight, we have been a bit puzzled that GAL17, which introduces a $\varphi$ preference, is not significantly different from METAL or the Siepmann and Sprik potential, where this dependence is missing for a single molecule. At second thought however, this can be explained as follows: the hydrogen repulsion introduced in Eq. 3 serves to push the hydrogen "up", away from the surface. At the Pt/$H_2O$ interface, the same effect can be obtained through the interaction with other water molecules: the hydrogen atoms are charged and will therefore interact with water molecules from the second layer and/or water molecules within the same layer. Hence, hydrogens will be dissuaded from pointing towards the surface due to competition. Nevertheless, we anticipate that the fine structure, such as corrugation and correlations between $\theta$ and $\varphi$, are affected by the physically motivated repulsion between hydrogen atoms and the surface.

Having mentioned the competition between water–water and water–surface interaction, we would like to emphasize the importance of the uncertainty associated with the water

model: since the interfacial structure is due to a balance between the energy of a water molecule at the interface and its energy in the bulk solution, it is an open question to which extent this difference is significant enough to be robust with respect to changes in the water model that mainly affect the water–water interactions. Hence, we have performed additional computations (see Figure S5 in the SI) by replacing the TIP4Pew water model by TIP5P and OPC, which are, according to Figure 7 the two extremes for weak and strong water–water interactions, respectively. We show in the SI that even though GAL17 and vsGAL17 are fairly similar for the single water molecule adsorption modes and for the ice-like layers, the results varying the water model and the water–surface interactions fail to provide fully consistent results for the angular distributions.

Hence, we conclude that the greatest caution should be applied when deriving conclusions about the "real" water/metal interfacial structure from either short AIMD or long MM simulations: The relaxation times at the Pt(111)/water interface are high[66] and, nevertheless, the energetic balance between water at the interface and water in bulk solution seems to be too subtle to produce clear-cut and robust interfacial characteristics.

# 5 Conclusion

We have presented a novel force field form for the interaction of water with Pt(111) to capture the angular dependence and surface corrugation. The 12 parameters of the GAL17 force field have been fitted to 210 DFT adsorption energies of water on a Pt(111) surface. The accuracy of GAL17 and several force fields from the literature have been compared for 802 adsorption energies on Pt(111), 52 geometries derived from ice-like layers and an MD simulation of a Pt(111)/water interface, for which we have also presented a 10 ps first principles trajectory. In all cases, GAL17 shows a better agreement with the DFT results than its predecessors. In particular, the adsorption energies of a single water molecule are reproduced with an RMSD of only 2 kcal $mol^{-1}$, while defective ice-like layers are within 4 kcal $mol^{-1}$ per $H_2O$ of the DFT

reference energies. Using this force field, we confirm that equilibration time of the interfacial water is much slower (by two orders of magnitude) than that of bulk water. Moreover, by assessing the combination of GAL17 with different water models, we demonstrate that the fine structure of the interface is very sensitive to the competition between platinum – water and water – water interactions. Hence, we suggest that force fields should only be used to generate relevant configurations that are, subsequently, reassessed at the DFT level in order to gain insight into the "true" nature of the interface, while also keeping in mind the shortcomings of DFT. However, since GAL17 is more accurate than other published force fields, it is a very promising step towards the assessment of MM based solvation free energies at the interface, which are particularly relevant in heterogeneous catalysis.

## Acknowledgement

The authors thank D. Golze for providing input files and equilibrated structures of the IC-QM/MM simulations and T. Jiang for some analysis scripts for the interface. Computational resources were generously provided by the mesocenter PSMN. This work was also granted access to the HPC resources of CINES and IDRIS under the allocation 2014-080609 and A0010810119 made by GENCI. The PHC Germaine de Staël program "Reactivity at the solid/liquid interface: Better simulation for a better comprehension", number 30617PA, is acknowledged for supporting the collaboration between CM and MI. This work benefited from the support of the project MuSiC ANR-14-CE06-0030 of the French National Research Agency (ANR). This research was also supported by the National Science Foundation (Grant number CHE-1416571) and used resources at the San Diego Supercomputer Center through the Extreme Science and Engineering Discovery Environment (XSEDE), which is supported by the National Science Foundation (Grant No. ACI-1053575, allocation TG-CHE130010).

## Supporting Information Available

The supporting information contains an archive of geometries, including the 802 water configurations on a p(3x3) unit cell, the 52 geometries derived from the ice-like water layers and the initial structure for the Pt(111)/$H_2O$ interface, together with a list of PBE-dDsC reference adsorption energies. Furthermore, additional Figures are provided, illustrating the Pt-O LJ interaction for various models and the evolution of the histograms of different angles with simulation time and as a function of the water model.

This material is available free of charge via the Internet at `http://pubs.acs.org/`.

## References


(1) Norskov, J. K.; Bligaard, T.; Rossmeisl, J.; Christensen, C. H. Towards the computational design of solid catalysts. *Nat Chem* **2009**, *1*, 37.

(2) van Santen, R. A.; Sautet, P. Conclusion: Challenges to Computational Catalysis. *Computational Methods in Catalysis and Materials Science: An Introduction for Scientists and Engineers* **2009**, 441.

(3) Calle-Vallejo, F.; Tymoczko, J.; Colic, V.; Vu, Q. H.; Pohl, M. D.; Morgenstern, K.; Loffreda, D.; Sautet, P.; Schuhmann, W.; Bandarenka, A. S. Finding optimal surface sites on heterogeneous catalysts by counting nearest neighbors. *Science* **2015**, *350*, 185.

(4) Alonso, D. M.; Wettstein, S. G.; Dumesic, J. A. Gamma-valerolactone, a sustainable platform molecule derived from lignocellulosic biomass. *Green Chem.* **2013**, *15*, 584.

(5) Besson, M.; Gallezot, P.; Pinel, C. Conversion of Biomass into Chemicals over Metal Catalysts. *Chem Rev* **2014**, *114*, 1827, PMID: 24083630.

(6) Benjamin, I. Chemical Reactions and Solvation at Liquid Interfaces: A Microscopic Perspective. *Chem Rev* **1996**, *96*, 1449.

(7) Hakkinen, H. The gold-sulfur interface at the nanoscale. *Nat Chem* **2012**, *4*, 443.

(8) Akpa, B. S.; D'Agostino, C.; Gladden, L. F.; Hindle, K.; Manyar, H.; McGregor, J.; Li, R.; Neurock, M.; Sinha, N.; Stitt, E. H.; Weber, D.; Zeitler, J. A.; Rooney, D. W. Solvent effects in the hydrogenation of 2-butanone. *J Catal* **2012**, *289*, 30.

(9) Michel, C.; Zaffran, J.; Ruppert, A. M.; Matras-Michalska, J.; Jedrzejczyk, M.; Grams, J.; Sautet, P. Role of water on metal catalyst performance for ketone hydrogenation. A joint experimental and theoretical study on levulinic acid conversion into gamma-valerolactone. *Chem. Comm.* **2014**, *50*, 12450.

(10) Michel, C.; Gallezot, P. Why Is Ruthenium an Efficient Catalyst for the Aqueous-Phase Hydrogenation of Biosourced Carbonyl Compounds? *ACS Catal* **2015**, *5*, 4130.

(11) Zaffran, J.; Michel, C.; Delbecq, F.; Sautet, P. Towards more accurate prediction of activation energies for polyalcohol dehydrogenation on transition metal catalysts in water. *Catal Sci Technol* **2016**, *6*, 6615.

(12) Bellarosa, L.; Garcia-Muelas, R.; Revilla-Lopez, G.; Lopez, N. Diversity at the Water-Metal Interface: Metal, Water Thickness, and Confinement Effects. *ACS Cent Sci* **2016**, *2*, 109.

(13) de Morais, R. F.; Kerber, T.; Calle-Vallejo, F.; Sautet, P.; Loffreda, D. Capturing Solvation Effects at a Liquid/Nanoparticle Interface by Ab Initio Molecular Dynamics: Pt201 Immersed in Water. *Small* **2016**, *12*, 5312.

(14) Sakong, S.; Forster-Tonigold, K.; Gross, A. The structure of water at a Pt(111) electrode and the potential of zero charge studied from first principles. *J Chem Phys* **2016**, *144*, 194701.

(15) Cheng, T.; Xiao, H.; Goddard, W. A. Full atomistic reaction mechanism with kinetics for CO reduction on Cu(100) from ab initio molecular dynamics free-energy calculations at 298 K. *Proc Natl Acad Sci* **2017**, *114*, 1795.

(16) Le, J.; Iannuzzi, M.; Cuesta, A.; Cheng, J. Determining Potentials of Zero Charge of Metal Electrodes versus the Standard Hydrogen Electrode from Density-Functional-Theory-Based Molecular Dynamics. *Phys Rev Lett* **2017**, *119*, 016801.

(17) Bulo, R. E.; Michel, C.; Fleurat-Lessard, P.; Sautet, P. Multiscale Modeling of Chemistry in Water: Are We There Yet? *J Chem Theory Comput* **2013**, *9*, 5567.

(18) Boereboom, J. M.; Fleurat-Lessard, P.; Bulo, R. E. Explicit Solvation Matters: Performance of QM/MM Solvation Models in Nucleophilic Addition. *J. Chem. Theory Comput.* **0**, *0*, doi:10.1021/acs.jctc.7b01206, PMID: 29438621.

(19) Tomasi, J.; Persico, M. Molecular Interactions in Solution: An Overview of Methods Based on Continuous Distributions of the Solvent. *Chem Rev* **1994**, *94*, 2027.

(20) Petrosyan, S. A.; Rigos, A. A.; Arias, T. A. Joint Density-Functional Theory: Ab Initio Study of Cr2O3 Surface Chemistry in Solution. *J Phys Chem B* **2005**, *109*, 15436.

(21) Andreussi, O.; Dabo, I.; Marzari, N. Revised self-consistent continuum solvation in electronic-structure calculations. *J Chem Phys* **2012**, *136*, 064102.

(22) Ringe, S.; Oberhofer, H.; Hille, C.; Matera, S.; Reuter, K. Function-Space-Based Solution Scheme for the Size-Modified Poisson-Boltzmann Equation in Full-Potential DFT. *J Chem Theory Comput* **2016**, *12*, 4052.

(23) Mathew, K.; Sundararaman, R.; Letchworth-Weaver, K.; Arias, T. A.; Hennig, R. G. Implicit solvation model for density-functional study of nanocrystal surfaces and reaction pathways. *J Chem Phys* **2014**, *140*, 084106.

(24) Hutter, J.; Iannuzzi, M.; Schiffmann, F.; VandeVondele, J. CP2K: atomistic simulations of condensed matter systems. *WIREs Comput Mol Sci* **2014**, *4*, 15.

(25) Mathew, K.; Hennig, R., R. G. Sundararaman; Letchworth-Weaver, K.; Schwarz, K. A.; Gunceler, D.; Ozhabes, Y.; Arias, T. JDFTx: software for joint density-functional theory. *ArXiv e-prints* **2017**, 1708.03621.

(26) Andreussi, O.; Nattino, F. ENVIRON. *http://www.quantum-environment.org/releases.html* **2017**,

(27) Saleheen, M.; Heyden, A. Liquid-Phase Modeling in Heterogeneous Catalysis. *ACS Catalysis* **2018**, *8*, 2188.

(28) Desai, S. K.; Pallassana, V.; Neurock, M. A Periodic Density Functional Theory Analysis of the Effect of Water Molecules on Deprotonation of Acetic Acid over Pd(111). *J Phys Chem B* **2001**, *105*, 9171.

(29) Michel, C.; Auneau, F.; Delbecq, F.; Sautet, P. C-H versus O-H Bond Dissociation for Alcohols on a Rh(111) Surface: A Strong Assistance from Hydrogen Bonded Neighbors. *ACS Catal* **2011**, *1*, 1430.

(30) Arnadottir, L.; Stuve, E. M.; Jonsson, H. The effect of coadsorbed water on the stability, configuration and interconversion of formyl (HCO) and hydroxymethylidyne (COH) on platinum (111). *Chem Phys Lett* **2012**, *541*, 32.

(31) Pliego, J. R.; Riveros, J. M. The Cluster-Continuum Model for the Calculation of the Solvation Free Energy of Ionic Species. *J Phys Chem A* **2001**, *105*, 7241.

(32) Asthagiri, D.; Pratt, L. R.; Ashbaugh, H. S. Absolute hydration free energies of ions, ion-water clusters, and quasichemical theory. *J Chem Phys* **2003**, *119*, 2702.

(33) Bryantsev, V. S.; Diallo, M. S.; Goddard III, W. A. Calculation of Solvation Free

Energies of Charged Solutes Using Mixed Cluster/Continuum Models. *J Phys Chem B* **2008**, *112*, 9709.

(34) Wang, H.-F.; Liu, Z.-P. Formic Acid Oxidation at Pt/H2O Interface from Periodic DFT Calculations Integrated with a Continuum Solvation Model. *J Phys Chem C* **2009**, *113*, 17502.

(35) Cao, D.; Lu, G. Q.; Wieckowski, A.; Wasileski, S. A.; Neurock, M. Mechanisms of methanol decomposition on platinum: A combined experimental and ab initio approach. *J Phys Chem B* **2005**, *109*, 11622.

(36) Wasileski, S. A.; Janik, M. J. A first-principles study of molecular oxygen dissociation at an electrode surface: a comparison of potential variation and coadsorption effects. *Phys Chem Chem Phys* **2008**, *10*, 3613.

(37) Zope, B. N.; Hibbitts, D. D.; Neurock, M.; Davis, R. J. Reactivity of the Gold/Water Interface During Selective Oxidation Catalysis. *Science* **2010**, *330*, 74.

(38) Hibbitts, D. D.; Neurock, M. Influence of oxygen and pH on the selective oxidation of ethanol on Pd catalysts. *J Catal* **2013**, *299*, 261.

(39) Revilla-Lopez, G.; Lopez, N. A unified study for water adsorption on metals: meaningful models from structural motifs. *Phys. Chem. Chem. Phys.* **2014**, *16*, 18933.

(40) Ogasawara, H.; Brena, B.; Nordlund, D.; Nyberg, M.; Pelmenschikov, A.; Pettersson, L. G. M.; Nilsson, A. Structure and Bonding of Water on Pt(111). *Phys Rev Lett* **2002**, *89*, 276102.

(41) Michaelides, A.; Ranea, V. A.; de Andres, P. L.; King, D. A. General Model for Water Monomer Adsorption on Close-Packed Transition and Noble Metal Surfaces. *Phys Rev Lett* **2003**, *90*, 216102.

(42) Bjorneholm, O.; Hansen, M. H.; Hodgson, A.; Liu, L.-M.; Limmer, D. T.; Michaelides, A.; Pedevilla, P.; Rossmeisl, J.; Shen, H.; Tocci, G.; Tyrode, E.; Walz, M.-M.; Werner, J.; Bluhm, H. Water at Interfaces. *Chem Rev* **2016**, *116*, 7698.

(43) Davda, R. R.; Shabaker, J. W.; Huber, G. W.; Cortright, R. D.; Dumesic, J. A. A review of catalytic issues and process conditions for renewable hydrogen and alkanes by aqueous-phase reforming of oxygenated hydrocarbons over supported metal catalysts. *Applied Catalysis B: Environmental* **2005**, *56*, 171.

(44) Liu, J.; Cao, X.-M.; Hu, P. Density functional theory study on the activation of molecular oxygen on a stepped gold surface in an aqueous environment: a new approach for simulating reactions in solution. *Phys Chem Chem Phys* **2014**, *16*, 4176, OO.

(45) Gu, G. H.; Schweitzer, B.; Michel, C.; Steinmann, S. N.; Sautet, P.; Vlachos, D. G. Group Additivity for Aqueous Phase Thermochemical Properties of Alcohols on Pt(111). *J Phys Chem C* **2017**, 10.1021/acs.jpcc.7b07340.

(46) Iyemperumal, S. K.; Deskins, N. A. Evaluating Solvent Effects at the Aqueous/Pt(111) Interface. *ChemPhysChem* **2017**, *18*, 2171–2190.

(47) Kovalenko, A.; Hirata, F. Self-consistent description of a metal-water interface by the Kohn-Sham density functional theory and the three-dimensional reference interaction site model. *J Chem Phys* **1999**, *110*, 10095.

(48) Faheem, M.; Heyden, A. Hybrid Quantum Mechanics/Molecular Mechanics Solvation Scheme for Computing Free Energies of Reactions at Metal-Water Interfaces. *J Chem Theory Comput* **2014**, *10*, 3354.

(49) Bodenschatz, C. J.; Sarupria, S.; Getman, R. B. Molecular-Level Details about Liquid $H_2O$ Interactions with CO and Sugar Alcohol Adsorbates on Pt(111) Calculated Using Density Functional Theory and Molecular Dynamics. *J Phys Chem C* **2015**, *119*, 13642.

(50) Lim, H.-K.; Lee, H.; Kim, H. A Seamless Grid-Based Interface for Mean-Field QM/MM Coupled with Efficient Solvation Free Energy Calculations. *J Chem Theory Comput* **2016**, *12*, 5088.

(51) Steinmann, S. N.; Sautet, P.; Michel, C. Solvation free energies for periodic surfaces: comparison of implicit and explicit solvation models. *Phys Chem Chem Phys* **2016**, *18*, 31850.

(52) Schravendijk, P.; van der Vegt, N.; Delle Site, L.; Kremer, K. Dual-Scale Modeling of Benzene Adsorption onto Ni(111) and Au(111) Surfaces in Explicit Water. *ChemPhysChem* **2005**, *6*, 1866.

(53) Lee, M.-S.; Peter McGrail, B.; Rousseau, R.; Glezakou, V.-A. Structure, dynamics and stability of water/scCO2/mineral interfaces from ab initio molecular dynamics simulations. *Sci. Rep.* **2015**, *5*, 14857.

(54) Cantu, D. C.; Wang, Y.-G.; Yoon, Y.; Glezakou, V.-A.; Rousseau, R.; Weber, R. S. Heterogeneous catalysis in complex, condensed reaction media. *Catal Today* **2017**, *289*, 231.

(55) Wertz, D. H. Relationship between the gas-phase entropies of molecules and their entropies of solvation in water and 1-octanol. *J Am Chem Soc* **1980**, *102*, 5316.

(56) Kelly, E.; Seth, M.; Ziegler, T. Calculation of Free Energy Profiles for Elementary Bimolecular Reactions by ab Initio Molecular Dynamics: Sampling Methods and Thermostat Considerations. *J Phys Chem A* **2004**, *108*, 2167.

(57) Toney, M. F.; Howard, J. N.; Richer, J.; Borges, G. L.; Gordon, J. G.; Melroy, O. R.; Wiesler, D. G.; Yee, D.; Sorensen, L. B. Voltage-dependent ordering of water molecules at an electrode-electrolyte interface. *Nature* **1994**, *368*, 444.

(58) Schiros, T.; Andersson, K. J.; Pettersson, L. G. M.; Nilsson, A.; Ogasawara, H. Chemical bonding of water to metal surfaces studied with core-level spectroscopies. *Journal of Electron Spectroscopy and Related Phenomena* **2010**, *177*, 85.

(59) Velasco-Velez, J.-J.; Wu, C. H.; Pascal, T. A.; Wan, L. F.; Guo, J.; Prendergast, D.; Salmeron, M. The structure of interfacial water on gold electrodes studied by x-ray absorption spectroscopy. *Science* **2014**, *346*, 831.

(60) Spohr, E.; Heinzinger, K. Molecular dynamics simulation of a water/metal interface. *Chem Phys Lett* **1986**, *123*, 218.

(61) Spohr, E.; Heinzinger, K. A Molecular Dynamics Study on the Water/Metal Interfacial Potential. *Ber Bunsenges Phys Chem* **1988**, *92*, 1358.

(62) Spohr, E. Computer simulation of the water/platinum interface. *J Phys Chem* **1989**, *93*, 6171.

(63) Zhu, S.; Philpott, M. R. Interaction of water with metal surfaces. *J Chem Phys* **1994**, *100*, 6961.

(64) Siepmann, J. I.; Sprik, M. Influence of surface topology and electrostatic potential on water/electrode systems. *J Chem Phys* **1995**, *102*, 511.

(65) Iori, F.; Di Felice, R.; Molinari, E.; Corni, S. GolP: An atomistic force-field to describe the interaction of proteins with Au(111) surfaces in water. *J Comput Chem* **2009**, *30*, 1465.

(66) Limmer, D. T.; Willard, A. P.; Madden, P.; Chandler, D. Hydration of metal surfaces can be dynamically heterogeneous and hydrophobic. *Proc Natl Acad Sci U S A* **2013**, *110*, 4200.

(67) Li, X.; Agren, H. Molecular Dynamics Simulations Using a Capacitance-Polarizability Force Field. *J Phys Chem C* **2015**, *119*, 19430.

(68) Natarajan, S. K.; Behler, J. Neural network molecular dynamics simulations of solid-liquid interfaces: water at low-index copper surfaces. *Phys Chem Chem Phys* **2016**, *18*, 28704.

(69) Berg, A.; Peter, C.; Johnston, K. Evaluation and Optimization of Interface Force Fields for Water on Gold Surfaces. *J. Chem. Theory Comput.* **2017**, *13*, 5610–5623, PMID: 28992416.

(70) Wang, Y.; Bowman, J. M. Ab initio potential and dipole moment surfaces for water. II. Local-monomer calculations of the infrared spectra of water clusters. *J Chem Phys* **2011**, *134*, 154510.

(71) Medders, G. R.; Babin, V.; Paesani, F. Development of a "First-Principles" Water Potential with Flexible Monomers. III. Liquid Phase Properties. *J Chem Theory Comput* **2014**, *10*, 2906.

(72) Perdew, J. P.; Burke, K.; Ernzerhof, M. Generalized Gradient Approximation Made Simple. *Phys Rev Lett* **1996**, *77*, 3865.

(73) Steinmann, S. N.; Corminboeuf, C. Comprehensive Benchmarking of a Density-Dependent Dispersion Correction. *J Chem Theory Comput* **2011**, *7*, 3567.

(74) Gautier, S.; Steinmann, S. N.; Michel, C.; Fleurat-Lessard, P.; Sautet, P. Molecular adsorption at Pt(111). How accurate are DFT functionals? *Phys Chem Chem Phys* **2015**, *17*, 28921.

(75) Holloway, S.; Bennemann, K. H. Study of water adsorption on metal surfaces. **1980**, *101*, 327.

(76) Yeh, K.-Y.; Janik, M. J.; Maranas, J. K. Molecular dynamics simulations of an electrified water/Pt(111) interface using point charge dissociative water. **2013**, *101*, 308.

(77) D.A. Case, D.S. Cerutti, T.E. Cheatham, III, T.A. Darden, R.E. Duke, T.J. Giese, H. Gohlke, A.W. Goetz, D. Greene, N. Homeyer, S. Izadi, A. Kovalenko, T.S. Lee, S. LeGrand, P. Li, C. Lin, J. Liu, T. Luchko, R. Luo, D. Mermelstein, K.M. Merz, G. Monard, H. Nguyen, I. Omelyan, A. Onufriev, F. Pan, R. Qi, D.R. Roe, A. Roitberg, C. Sagui, C.L. Simmerling, W.M. Botello-Smith, J. Swails, R.C. Walker, J. Wang, R.M. Wolf, X. Wu, L. Xiao, D.M. York and P.A. Kollman (2017), AMBER 2017, University of California, San Francisco.

(78) Heinz, H.; Vaia, R. A.; Farmer, B. L.; Naik, R. R. Accurate Simulation of Surfaces and Interfaces of Face-Centered Cubic Metals Using 12-6 and 9-6 Lennard-Jones Potentials. *J Phys Chem C* **2008**, *112*, 17281.

(79) Golze, D.; Iannuzzi, M.; Nguyen, M.-T.; Passerone, D.; Hutter, J. Simulation of Adsorption Processes at Metallic Interfaces: An Image Charge Augmented QM/MM Approach. *J Chem Theory Comput* **2013**, *9*, 5086.

(80) Willard, A. P.; Limmer, D. T.; Madden, P. A.; Chandler, D. Characterizing heterogeneous dynamics at hydrated electrode surfaces. *J Chem Phys* **2013**, *138*, 184702.

(81) van Duin,; Adri C., T.; Bryantsev, V. S.; Diallo, M. S.; Goddard, W. A.; Rahaman, O.; Doren, D. J.; Raymand, D.; Hermansson, K. Development and Validation of a ReaxFF Reactive Force Field for Cu Cation/Water Interactions and Copper Metal/Metal Oxide/Metal Hydroxide Condensed Phases. *J Phys Chem A* **2010**, *114*, 9507.

(82) Iori, F.; Corni, S. Including image charge effects in the molecular dynamics simulations of molecules on metal surfaces. *J Comput Chem* **2008**, *29*, 1656.

(83) Steinmann, S. N.; Fleurat-Lessard, P.; Götz, A. W.; Michel, C.; Ferreira de Morais, R.; Sautet, P. Molecular mechanics models for the image charge, a comment on "including image charge effects in the molecular dynamics simulations of molecules on metal surfaces". *J Comput Chem* **2017**, *38*, 2127.

(84) Corni, S. Reply to "Molecular mechanics models for the image charge". *J Comput Chem* **2017**, *38*, 2130.

(85) Meng, S.; Wang, E. G.; Gao, S. Water adsorption on metal surfaces: A general picture from density functional theory studies. *Phys. Rev. B* **2004**, *69*, 195404.

(86) Cicero, G.; Calzolari, A.; Corni, S.; Catellani, A. Anomalous Wetting Layer at the Au(111) Surface. *J. Phys. Chem. Lett.* **2011**, *2*, 2582.

(87) Michel, C.; Goltl, F.; Sautet, P. Early stages of water/hydroxyl phase generation at transition metal surfaces - synergetic adsorption and O-H bond dissociation assistance. *Phys Chem Chem Phys* **2012**, *14*, 15286.

(88) Medders, G. R.; Götz, A. W.; Morales, M. A.; Bajaj, P.; Paesani, F. On the representation of many-body interactions in water. *J Chem Phys* **2015**, *143*, 104102.

(89) Reddy, S. K.; Straight, S. C.; Bajaj, P.; Pham, C. H.; Riera, M.; Moberg, D. R.; Morales, M. A.; Knight, C.; Götz, A. W.; Paesani, F. On the accuracy of the MB-pol many-body potential for water: Interaction energies, vibrational frequencies, and classical thermodynamic and dynamical properties from clusters to liquid water and ice. *J Chem Phys* **2016**, *145*, 194504.

(90) Mitsui, T.; Rose, M. K.; Fomin, E.; Ogletree, D. F.; Salmeron, M. Water Diffusion and Clustering on Pd(111). *Science* **2002**, *297*, 1850.

(91) Le Roy, R. J.; Dattani, N. S.; Coxon, J. A.; Ross, A. J.; Crozet, P.; Linton, C. Accurate analytic potentials for $Li_2(X^1\Sigma_g^+)$ and $Li_2(A^1\Sigma_u^+)$ from 2 to 90 Å, and the radiative lifetime of Li(2p). *J. Chem. Phys.* **2009**, *131*, 204309.

(92) Kresse, G.; Hafner, J. Ab initio molecular dynamics for liquid metals. *Phys Rev B* **1993**, *47*, 558.

(93) Kresse, G.; Furthmuller, J. Efficient iterative schemes for ab initio total-energy calculations using a plane-wave basis set. *Phys Rev B* **1996**, *54*, 11169.

(94) Blochl, P. E. Projector augmented-wave method. *Phys Rev B* **1994**, *50*, 17953.

(95) Kresse, G.; Joubert, D. From ultrasoft pseudopotentials to the projector augmented-wave method. *Phys Rev B* **1999**, *59*, 1758.

(96) Grimme, S.; Antony, J.; Ehrlich, S.; Krieg, H. A consistent and accurate ab initio parametrization of density functional dispersion correction (DFT-D) for the 94 elements H-Pu. *J Chem Phys* **2010**, *132*, 154104.

(97) Darden, T.; York, D.; Pedersen, L. Particle mesh Ewald: An Nlog(N) method for Ewald sums in large systems. *J. Chem. Phys.* **1993**, *98*, 10090.

(98) Berendsen, H. J. C.; Postma, J. P. M.; Gunsteren, W. F. v.; DiNola, A.; Haak, J. R. Molecular dynamics with coupling to an external bath. *J Chem Phys* **1984**, *81*, 3684.

(99) Miyamoto, S.; Kollman, P. A. Settle: An analytical version of the SHAKE and RATTLE algorithm for rigid water models. *J. Comput. Chem.* **1992**, *13*, 952.

(100) VandeVondele, J.; Hutter, J. An efficient orbital transformation method for electronic structure calculations. *J Chem Phys* **2003**, *118*, 4365.

(101) Izvekov, S.; Parrinello, M.; Burnham, C. J.; Voth, G. A. Effective force fields for condensed phase systems from ab initio molecular dynamics simulation: A new method for force-matching. *J. Chem. Phys.* **2004**, *120*, 10896.

(102) Soler, J. M.; Artacho, E.; Gale, J. D.; García, A.; Junquera, J.; Ordejón, P.; Sánchez-Portal, D. The SIESTA method for ab initio order- N materials simulation. *J Phys : Condens Matter* **2002**, *14*, 2745.

(103) Konig, G.; Hudson, P. S.; Boresch, S.; Woodcock, H. L. Multiscale Free Energy Simulations: An Efficient Method for Connecting Classical MD Simulations to QM or

QM/MM Free Energies Using Non-Boltzmann Bennett Reweighting Schemes. *J Chem Theory Comput* **2014**, *10*, 1406.

(104) Cave-Ayland, C.; Skylaris, C.-K.; Essex, J. W. A Monte Carlo Resampling Approach for the Calculation of Hybrid Classical and Quantum Free Energies. *J Chem Theory Comput* **2017**, *13*, 415.

(105) Raghavan, K.; Foster, K.; Motakabbir, K.; Berkowitz, M. Structure and dynamics of water at the Pt(111) interface: Molecular dynamics study. *J Chem Phys* **1991**, *94*, 2110.

(106) van Duin,; Adri C., T.; Dasgupta, S.; Lorant, F.; Goddard, W. A. ReaxFF: A Reactive Force Field for Hydrocarbons. *J Phys Chem A* **2001**, *105*, 9396.

(107) Jorgensen, W. L.; Chandrasekhar, J.; Madura, J. D.; Impey, R. W.; Klein, M. L. Comparison of simple potential functions for simulating liquid water. *J Chem Phys* **1983**, *79*, 926.

(108) Horn, H. W.; Swope, W. C.; Pitera, J. W.; Madura, J. D.; Dick, T. J.; Hura, G. L.; Head-Gordon, T. Development of an improved four-site water model for biomolecular simulations: TIP4P-Ew. *J Chem Phys* **2004**, *120*, 9665.

(109) Mahoney, M. W.; Jorgensen, W. L. A five-site model for liquid water and the reproduction of the density anomaly by rigid, nonpolarizable potential functions. *J Chem Phys* **2000**, *112*, 8910.

(110) Berendsen, H. J. C.; Grigera, J. R.; Straatsma, T. P. The missing term in effective pair potentials. *J Phys Chem* **1987**, *91*, 6269.

(111) Izadi, S.; Anandakrishnan, R.; Onufriev, A. V. Building Water Models: A Different Approach. *J Phys Chem Lett* **2014**, *5*, 3863.

(112) Vignola, E.; Steinmann, S. N.; Vandegehuchte, B. D.; Curulla, D.; Stamatakis, M.; Sautet, P. A machine learning approach to graph-theoretical cluster expansions of the energy of adsorbate layers. *J Chem Phys* **2017**, *147*, 054106.

(113) Chen, J.; Zen, A.; Brandenburg, J. G.; Alfe, D.; Michaelides, A. Evidence for stable square ice from quantum Monte Carlo. *Phys. Rev. B* **2016**, *94*, 220102.

(114) Tarmyshov, K. B.; Mueller-Plathe, F. Interface between platinum(111) and liquid isopropanol (2-propanol): A model for molecular dynamics studies. *J Chem Phys* **2007**, *126*, 074702.

# Graphical TOC Entry